Solid-that-flows picture of glass-forming liquids

Jeppe C. Dyre[1]

[1] *"Glass and Time", IMFUFA, Dept. of Sciences, Roskilde University, P. O. Box 260, DK-4000 Roskilde, Denmark*

(Dated: November 27, 2023)

This article reviews arguments that glass-forming liquids are different from those of standard liquid-state theory. The latter typically have a viscosity in the mPa·s range and relaxation times of order picoseconds, while these numbers grow dramatically and become $10^{12} - 10^{15}$ times larger for liquids cooled toward the glass transition. This translates into a qualitative difference, and below the "solidity length" which is of order one micron at the glass transition, a glass-forming liquid behaves much like a solid. Recent numerical evidence for the solidity of ultraviscous liquids is reviewed, and experimental consequences are discussed in relation to dynamic heterogeneity, frequency-dependent linear-response functions, and the temperature dependence of the average relaxation time.

I. INTRODUCTION

It is common knowledge that liquids flow and solids do not. From a scientific point of view, however, the distinction is not that straightforward because any solid does flow when subjected to an external force [1–7] while, on the other hand, an extremely viscous liquid only flows very slowly. Should one think of the latter as an "ordinary" liquid like water or a molten metal, merely with a much higher viscosity, or more as a solid that flows? This question is important for liquids approaching the glass transition where the viscosity is $10^{12} - 10^{15}$ times larger than that of an "ordinary" liquid (brief introductions to the glass transition are given in Refs. 8–12, more comprehensive reviews in Refs. 13–24).

Recall the three fundamental states of matter: gas, liquid, and solid. The gas and liquid phases are isotropic and translationally invariant on the macroscopic scale, while the solid phase is crystalline and breaks these symmetries. Thus gas and liquid appear to have most in common; indeed flow of both phases is described by the Navier-Stokes equation [25, 26]. On the other hand, it may be argued that liquids are more like solids by having roughly the same density and compressibility, an entropy closer to that of the solid phase, etc [27–30]. This semi-philosophical discussion relates to liquids in general, however, not to whether liquids differ qualitatively depending on their viscosity.

A glass is usually made by supercooling a liquid fast enough to avoid crystallization. It is a solid that has inherited the liquid's disorder and isotropy. While some substances like pure metals require extremely high cooling rates to form glasses, others, e.g., many organic liquids, are easily supercooled and in fact often difficult to crystallize. Because all substances can form glasses, glass may be regarded as the fourth state of conventional matter [11].

With only few exceptions like silicates, a liquid's viscosity η at the melting temperature T_m is within one or two orders of magnitude of that of water, $\eta \sim 10^{-3}$ Pa·s. Upon cooling the viscosity increases dramatically, and for typical cooling rates of order K/min one finds $\eta \sim 10^{12}$ Pa s at the glass transition temperature T_g. The glass transition is continuous and not a genuine phase transition, although T_g is fairly well defined for a given cooling rate (typically within 1%). At T_g the system falls out of metastable equilibrium because the time to reach equilibrium after an external disturbance, the so-called α relaxation time τ_α, exceeds the laboratory time scale. By the fluctuation-dissipation theorem τ_α is also the characteristic time of the equilibrium dynamics. This quantity is termed the Maxwell relaxation time, and in the simple Maxwell model of viscoelasticity [11, 31, 32] τ_α is given by

$$\tau_\alpha = \frac{\eta}{G_\infty} \tag{1}$$

where G_∞ is the high-frequency plateau shear modulus corresponding to MHz frequencies and above (sometimes denoted by G_p). In this expression the temperature dependence of G_∞ is insignificant, so upon cooling τ_α increases roughly in proportion to η. With $G_\infty \sim 10^9$ Pa the typical "ordinary" liquid viscosity 10^{-3} Pa·s corresponds to $\tau_\alpha \sim 10^{-12}$s, which is comparable to vibration (phonon) times. On the other hand, equating τ_α to the typical cooling time for producing a glass $\sim 10^3$ s leads to $\eta \sim 10^{12}$ Pa·s.

A note on terminology: The term "glass" is used below whenever a highly viscous liquid is not in thermodynamic equilibrium, while "liquid" is reserved to a system in (metastable) equilibrium, i.e., one that is fully characterized by pressure and temperature with no memory of its past. The terms "glass-forming liquid" and "ultraviscous liquid" are used synonymously reflecting the fact that once a liquid has been supercooled to the ultraviscous state by avoiding crystallization, glass formation is inevitable upon continued, sufficiently fast cooling.

II. THE PHYSICS OF ULTRAVISCOUS LIQUIDS

This section summarizes the relevant physics of standard liquid-state theory [33, 34] and argues that molec-

ular motion in a glass-forming liquid proceeds via rare "flow events" taking the system from one solid-like configuration to another. It depends on the length scale of observation, however, whether an ultraviscous liquid behaves as a *solid-that-flows* , and the "solidity length" below which this applies is identified (Sec. II D). Finally, the role of conservation laws is briefly reflected upon.

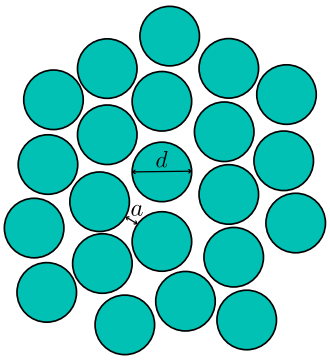

FIG. 1. Hard-sphere liquid in two dimensions. There are frequent collisions because the particles almost touch. For an order-of-magnitude estimate of the system's transport properties, however, one can assume that $a \sim d$.

A. "Ordinary" liquids

Consider a pure substance above its melting temperature. As a crude approximation one may adopt the hard-sphere (HS) model consisting of identical particles that do not interact, except by never overlapping (Fig. 1). Although this model is highly idealized, it is quite successful in reproducing the structure and dynamics of many liquids [33]. This applies also to systems with the attractions that are present in all real liquids. Temperature plays no role in the HS model except for determining the average particle velocity, i.e., the relevant time scale; the only nontrivial thermodynamic variable is the density (packing fraction). The HS model may be regarded as a mathematician's idealized liquid/gas; an alternative generic model in which temperature does play a role is the EXP system defined by the exponential pair potential [35–37].

In the HS liquid each particle is close to several others (Fig. 1). The frequent particle collisions result in an erratic motion. This is different from what happens in the gas phase in which the mean-free path between collisions is much larger than the particle diameter. It is useful to discuss the physics of the HS liquid in terms of three diffusion coefficients, the particle-diffusion coefficient $D_{\rm par}$, the heat-diffusion coefficient $D_{\rm heat}$, and the transverse-momentum diffusion coefficient $D_{\rm mom}$. The latter is the so-called kinematic viscosity ν of the Navier-Stokes equation, $D_{\rm mom} = \nu \equiv \eta/\rho$ in which ρ is the mass density [25]. $D_{\rm par}$ is defined from the long-time mean-square particle displacement via $\langle \Delta x^2(t) \rangle = 2D_{\rm par}t$. The heat-diffusion coefficient is defined as $D_{\rm heat} \equiv \lambda/c_V$ in which λ is the heat conductivity and c_V the specific heat per unit volume.

In the HS liquid these diffusion coefficients are of same order of magnitude. We write $A \sim B$ to indicate that A and B are within one or two decades of each other. That $D_{\rm heat} \sim D_{\rm mom}$ reflects the fact that any particle collision involves both a transfer of momentum and of energy. These two diffusion coefficients may be estimated as l^2/t in which l is the length involved and τ_α is roughly the time between collisions, i.e., $D_{\rm heat} \sim D_{\rm mom} \sim d^2/\tau_\alpha$ where d is the particle diameter. For $D_{\rm par}$ one estimates $D_{\rm par} \sim a^2/\tau_\alpha$ where a is the average distance between two neighboring particles. Although the HS liquid is characterized by $a < d$ implying that $D_{\rm par}$ is smaller than $D_{\rm heat}$ and $D_{\rm mom}$, one still has $D_{\rm par} \sim D_{\rm mom}$. In summary, the HS system – and by implication any "ordinary" liquid – is characterized by

$$D_{\rm par} \sim D_{\rm heat} \sim D_{\rm mom}\,. \tag{2}$$

Typical values are of order $10^{-7}\,{\rm m}^2/{\rm s}$, which may be arrived at from $D_{\rm par} \sim l^2/\tau_\alpha$ with $l \sim 10^{-10}$ m and $\tau_\alpha \sim 10^{-13}$ s or from $D_{\rm mom} = \eta/\rho$ with $\eta \sim 10^{-3}$ Pa·s and $\rho \sim 10^3\,{\rm kg/m}^3$.

B. Ultraviscous liquids

In equilibrium all atoms/molecules have velocities proportional to the square root of temperature, but this does not necessarily imply lasting particle displacement. In a crystal, for instance, all thermal motion goes into vibrations around the equilibrium positions. Intuitively, one expects the effective particle motion in an ultraviscous liquid to be minute, because in order to move a particle with a certain velocity, a force is required that is proportional to the viscosity. This is reflected in the Stokes-Einstein relation according to which the particle diffusion coefficient is inversely proportional to the viscosity [34, 38]. Although derived by reference to macroscopic hydrodynamics, the Stokes-Einstein relation works relatively well even on the molecular scale [39]. The relation is violated by 1-3 orders of magnitude for liquids approaching the glass transition [40–43], but this does not change the fact that when viscosity increases upon cooling, $D_{\rm par}$ decreases roughly as much, e.g., as $D_{\rm par} \propto \eta^{-0.9}$ [44]. Thus when the viscosity – and thereby $D_{\rm mom}$ – increases by a factor of 10^{15} by cooling from T_m to T_g, $D_{\rm par}$ at the same time decreases enormously. In contrast, the heat-diffusion coefficient changes only moderately [45]. We conclude that Eq. (2) for an ultraviscous liquid is replaced by

$$D_{\rm par} \ll D_{\rm heat} \ll D_{\rm mom}\,. \tag{3}$$

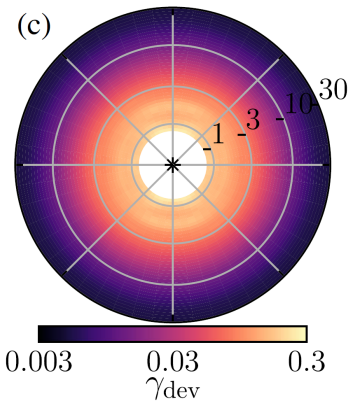

FIG. 2. Average deviatoric strain displacement around a flow event in simulations of a 2d polydisperse glass-forming liquid. The observed long-range decay $\propto 1/r^2$ is that predicted by solid-state elasticity theory [46]. Reproduced from Ref. 47.

C. Flow events

Since effective particle motion is exceedingly slow in an ultraviscous liquid while the velocities are not small, most motion must go into vibrations. Two possible scenarios can realize this. Either the vibrations take place around average positions that change continuously but very slowly. Alternatively, the vibrations are interrupted by sudden rare localized "flow events" that rearrange a handful of particles, with some effects also on their surroundings in the form of slight position adjustments. Experiments on colloidal [19], molecular [48], and metallic [49] glass-forming liquids, as well as computer simulations [50], favor the latter scenario.

In fact, it is an old idea that particle motion in a glass-forming liquid proceeds via flow events. In his seminal 1948 review Kauzmann referred to flow events as "jumps of molecular units of flow between different positions of equilibrium in the liquid's quasicrystalline lattice" [51]. Mooney in 1957 poetically referred to a flow event as "a quantum of liquid flow" [31], and many subsequent papers have embraced this picture of viscous liquid dynamics [52–57]. The physics, of course, lies in what determines the energy barriers for flow events and how these events correlate in space and time.

Why are flow events rare in an ultraviscous liquid? This was reflected upon by Goldstein in 1969 in a paper that remains a pleasure to read [58]. He identified Kauzmann's "positions of equilibrium" with minima of the potential-energy function. Flow events are rare because the barriers to be overcome going from one minimum to another are much larger than k_BT. Potential-energy minima are nowadays referred to as "inherent states" [59]. Goldstein's picture is that the dynamics of an ultraviscous liquid involves numerous vibrations around an inherent state like in a crystal. These vibrations do not contribute to the overall dynamics and may be eliminated by focusing on the "inherent dynamics" defined as the time sequence of inherent states [50, 60].

Accepting that an ultraviscous liquid may be regarded as a solid on a sufficiently short length scale, any flow event leads to minor deformations in its surroundings [61–63] as may be detected, e.g., by NMR experiments [64]. A flow event is not a linear perturbation and its effects are not easily predicted. Sufficiently far from the flow event, however, linear elasticity arguments may be referred to, and in three dimensions the induced particle motions scale as $1/r^2$ for $r \to \infty$ where r is the distance to the flow event [46] (Fig. 2). To show this one uses the mechanical-equilibrium requirement that the time-averaged force on each particle is zero both before and after a flow event, arguing as follows. Ignoring correlations to, and effects of, other flow events, a single flow event's effects on the surroundings may be reproduced by imagining external forces acting on a small surface surrounding it [65–67]. By momentum conservation, each of these forces leads to a momentum flow into the surroundings $\propto 1/r^2$ for $r \to \infty$. Since the forces sum to zero, this implies an overall momentum flow (stress tensor) that is the spatial derivative, i.e., $\propto 1/r^3$. According to elasticity theory [46], the stress tensor change is linearly related to the strain field, which is formed from derivatives of the displacement field that consequently scale as $\propto 1/r^2$ [68]. In two dimensions, the stress and strain fields induced by a flow event scale as $\propto 1/r^2$ for $r \to \infty$ and the particle displacements as $\propto 1/r$.

D. The solidity length

The arguments of Sec. II C suggest that the physics of an ultraviscous liquid is reminiscent to that of a crystal. Real-life solids are mostly crystalline with grain boundaries separating micrometer-sized or larger single crystals containing point defects. In thermal equilibrium a pure-substance solid is a single crystal with no line defects or grain boundaries, but a few point defects like vacancies and interstitials are always present at finite temperatures [69]. Point defects can jump to neighboring positions by overcoming a barrier much larger than k_BT.

In regard to ultraviscous liquids, we note that the effect of one flow event on its surroundings is not instantaneous, but propagates with a finite velocity. After a flow event, others will take place nearby that likewise send out spherical "waves" of minor particle adjustments. Far from the original flow event, the adjustments originating from many other flow events interfere with and increasingly smear out the effect of the original flow event. We proceed to estimate the length scale below which this does *not* happen, which defines the system's "solidity length" $l_{\rm s}$.

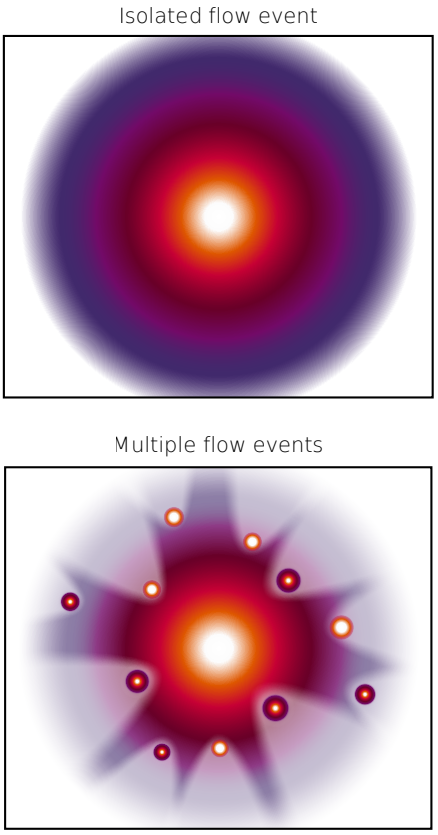

FIG. 3. A single isolated flow event and its screening by nearby subsequent flow events. The radius of the sphere inside which the effects of the original flow event are felt is the solidity length l_s.

As long as no other flow event has taken place within the "adjustment sphere" of one flow event, solid-state type arguments can be applied by reference to the inherent states before and after the event. However, when many other flow events have taken place within the sphere, each sending out its own disturbance wave, the effects of the original flow event are washed out (Fig. 3). To estimate l_s we assume that the average time between two flow events involving a given molecule is τ_α. If a is the average intermolecular distance, a sphere of radius l_s contains or order $N \cong (l_s/a)^3$ sites for potential flow events. Flow events are not independent and uncorrelated (Sec. IV A), but for simplicity we ignore this and estimate that the average time between two flow events within the sphere is τ_α/N. The solidity length is determined by requiring this to be the time it takes a sound wave to travel l_s, which is l_s/c where c is the sound velocity [70]. This leads to

$$l_s^4 \cong c\, a^3\, \tau_\alpha\,. \tag{4}$$

For an "ordinary" liquid the derivation makes little sense, but if one nevertheless substitutes $c \sim 10^3$ m/s, $a \sim 10^{-10}$ m, and $\tau_\alpha \sim 10^{-13}$ s into Eq. (4) the result is $l_s \sim 10^{-10}$ m. For a liquid approaching the glass transition, $\tau_\alpha \sim 10^2$ s leads to $l_s \sim 10^{-6}$ m. Note that this length is much larger than those discussed in connection with dynamic heterogeneities of glass-forming liquids [71–74]. Note also that the derivation of Eq. (4) is general and applies also for network-forming liquids like silica.

A single crystal with point defects also has a finite solidity length, but here the concept is not relevant because the crystal structure defines solid-like particle correlations over distances stretching to infinity. For an ultraviscous liquid, on the other hand, rigid distance correlations are only expected to apply below the solidity length.

Furukawa has argued that the length ξ defined by $\xi^4 \equiv a^4\tau_\alpha/\tau_0$, in which τ_0 is a microscopic time, is the characteristic length over which long-lived stress is sustained [75, 76]. He proposed that the ultraviscous liquid may be regarded as an ordinary liquid composed of clusters of size $\xi \simeq l_s$; in particular that standard hydrodynamics only applies on length scales above ξ. Much of the physics probed in experiments takes place below the solidity length, however. This is the case, e.g., for dielectric relaxation or NMR experiments probing a molecular average property. Actually, measuring a macroscopic dynamic property like the viscosity η becomes increasingly difficult as the glass transition is approached [77].

E. Conservation laws

Below the solidity length the laws of conservation of the number of particles, the momentum, and the energy play a role that is different from the case of "ordinary" liquids where these laws form the basis of hydrodynamics [6, 33, 39, 78, 79]. Consider first particle conservation. A molecular dynamics simulation keeps track of the individual particles, but things look different in a coarse-grained description based on a continuous density field $\rho(\mathbf{r}, t)$. This field is constant in time until it changes due to a flow event, a change that below the solidity length may be regarded as instantaneous. In general, flow events are not spherically symmetric (Sec. III B), but this assumption can be made for estimating the flow-event induced density changes. A spherically symmetric flow event leads to purely radial displacements in the surroundings $\propto 1/r^2$ (Sec. II C). The divergence of the displacement field determines the local density change [46] which is zero, compare Gauss' law for the point-charge electric field $\propto 1/r^2$. On the other hand, radial displacement can only take place if there is a density change at the flow-event center. If the density change, coarse-grained over a few molecular distances, is denoted by $\Delta\rho(\mathbf{r})$, for $|\mathbf{r} - \mathbf{r}_0| > a$ a flow event at $\mathbf{r}_0$ leads to

$$\Delta\rho(\mathbf{r}) = 0\ ,\ \Delta\rho(\mathbf{r}_0) \neq 0\,. \tag{5}$$

Comparing the situation before and after a flow event, local particle conservation is thus apparently violated. What happens is reminiscent of Hilbert's hotel, the full infinite hotel that hosts new arrivals by asking all guests to move to a room of one higher number.

Below the solidity length flow events may as mentioned be regarded as instantaneous. If all flow events are isotropic, the above leads to the following coarse-grained description with no visible trace of particle-number conservation,

$$\dot{\rho}(\mathbf{r},t) \;=\; \sum_j b_j \delta(\mathbf{r}-\mathbf{r}_j)\delta(t-t_j)\,. \qquad (6)$$

Here b_j is a dimensionless measure of the magnitude of a flow event at time t_j and position $\mathbf{r}_j$. Apparent density non-conservation holds also if the small advective density changes and the more realistic anisotropic Eshelby-type flow events [62, 65, 80] (see Sec. III A) are taken into account.

Below the solidity length mechanical equilibrium applies in the time between flow events, i.e., the time-averaged forces are zero. In a coarse-grained description this is expressed as zero divergence of the stress tensor, $\sigma_{\mu\nu}(\mathbf{r},t)$ [46]

$$\partial_\mu \sigma_{\mu\nu}(\mathbf{r},t) \;=\; 0 \qquad (7)$$

in which ∂_μ is the spatial derivative with respect to x_μ where $\mathbf{r} = (x_1, x_2, x_3)$. In this description the dynamics is regarded as a series of instantaneous transitions between states of mechanical equilibrium, each described by Eq. (7).

Momentum conservation thus plays little role in the dynamics below the solidity length. The situation is like that of point-defect motion in a crystal in which case one would never invoke momentum conservation. The same applies for energy conservation: In an ultraviscous liquid energy flow predominantly takes place via heat conduction, just like in a solid, and this process is irrelevant for the rate of flow events or for explaining how these correlate in space and time. Note that we are not suggesting that strict particle, momentum, or energy conservation is violated, merely that these conservation laws are irrelevant for the relevant coarse-grained description.

III. LEARNING FROM GLASSES

A liquid is *a priori* simpler than a glass, because the former is fully characterized by just two thermodynamic variables while there are infinitely many glasses, the properties of which reflect the formation history. Nevertheless, much has been learned from studies of glasses that is relevant for the liquid state. Initially, many simulations of glass properties focused on 2d glasses, but later works confirmed that the conclusions apply also in 3d.

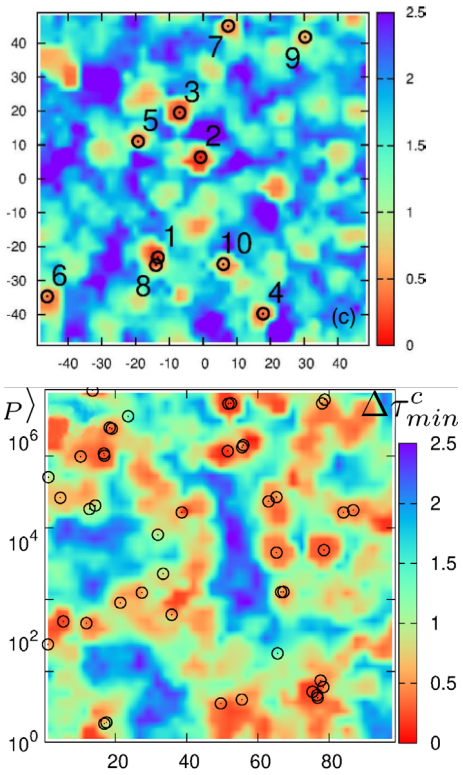

FIG. 4. Soft spots in glasses and liquids. (a) Softness probed as the local yield stress of a 2d binary Lennard-Jones glass in which reddish is soft and bluish is hard. The numbered points mark the sequence and location of plastic flow events when the system is sheared. Clearly, these are located at the soft spots. Reproduced from Ref. 81. (b) Analogous results for an equilibrium ultraviscous liquid in which softness is probed by the local yield stress of the system's inherent states, i.e., potential-energy minima. The circles mark the first 50 flow events. Like the plastic flow events of (a), these preferably take place at the soft spots. Reproduced from Ref. 82.

A. Flow events in plastic flows of glasses

When a glass is subjected to a gradual shear deformation, it eventually yields by deforming irreversibly [83–87]. The last 15 years has brought tremendous progress in the understanding of zero-temperature plastic flow of glasses [88], which proceeds as a sequence of sudden, localized flow events [89–91]. These do not take place at random locations, but at soft spots in the glass, compare Fig. 4(a) [92].

Different methods have been used with success for identifying soft spots [88]. An early approach was to look for atoms with a large vibrational mean-square displacement, a simple indicator that the potential is soft at the particle in question [93]. The mean local potential-energy fluctuation has also been used as soft-spot identifier [94]. The so-called local-yield-stress method considers a small sphere and constrains the outside system to

deform affinely such that only the atoms inside the sphere can relax when the system is shear deformed [81, 95]. Different sphere locations and shear-deformations are probed in order to identify the positions of the smallest local yield stresses. This method works well for identifying the sites of plastic rearrangement but requires knowledge of the interaction potentials. Methods for identifying sites for plastic flow events based purely on structural information have also been devised [96, 97] using, e.g., a mean-field caging potential [98] or machine-learning techniques [99, 100]. One method [99] defines "softness" as a weighted integral over local radial pair-correlation functions and optimize the weights for predicting sites of rearrangement by learning from plastic flows. The results obtained correlate well with those of the yield-stress method.

An alternative approach utilizes the fact that soft spots give rise to localized phonon modes, implying that the latter are good predictors for plasticity [101–105]. Low-energy localized vibrational modes may be identified by an anharmonic analysis of the potential-energy function, a clever method that avoids the hybridization with low-frequency sound-wave modes found by merely diagonalizing the Hessian [106].

To summarize, plastic flow takes place via sudden flow events. The physics is similar to what happens in an equilibrium ultraviscous liquid (Sec. II C) because flow events are also here located at "soft spots" (Fig. 4(b)). One difference is that the flow-event sequence of a zero-temperature plastic flow is deterministic, while the liquid's flow events are stochastic. Another difference is the lack of isotropy in a plastic flow, leading to preferred orientations of the Eshelby stress fields to which we now turn.

B. Strain and stress correlations in the liquid phase

We return in Sec. IV C to the idea that flow events are controlled by the system's elastic properties and focus next on another property of glasses, the fact that any flow event induces a quadrupolar stress-field change in the surroundings [107]. This is explained by the 1957 general theory of solid "inclusions" of Eshelby [65], which applies also to disordered solids because these are effectively homogeneous on long length scales. Eshelby calculated the long-ranged stress and strain changes of an inclusion by replacing it with localized forces in an elastic continuum. Each force gives rise to a momentum current into the solid, and since the forces sum to zero (Sec. II C), the result is a quadrupolar stress field [65, 80].

The obvious question is to which extent the long-ranged stress correlations of glasses [108] are seen also in glass-forming liquids [109–112]. One expects this to be the case below the solidity length because here the properties of the liquid's inherent states – each of which corresponds to a $T = 0$ glass – is inherited by the equilibrium liquid (Fig. 5). Thus long-ranged strain and stress correlations *a la* Eshelby are expected also in an ultraviscous liquid [109, 113–116]; for instance the average displacement probability generated by a flow event decays as $1/r^{5/2}$ for $r \to \infty$ [50, 70].

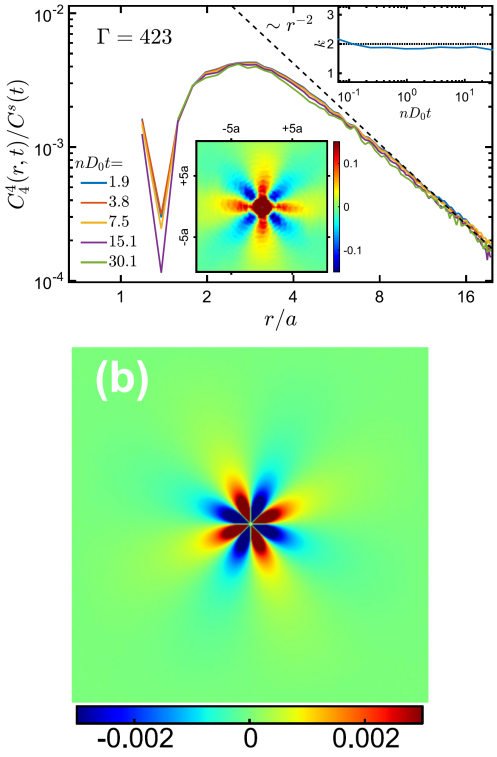

FIG. 5. Spatial strain and stress correlations in ultraviscous liquids. (a) Experimental data for the strain correlations in a 2d colloidal glass-forming liquid. The lower inset shows the spatial correlation function of the xy stain-tensor increase over a time $t \gg \tau_\alpha$. The curves are normalized spherical-harmonics projections of this function at different times, which are proportional to $1/r^2$ as predicted for Eshelby patterns in 2d [65, 80]. Reproduced from Ref. 63. (b) Stress-tensor correlations in a viscous 2d binary Lennard-Jones system. The figure shows the correlations between the normal-shear-stress increment correlations of a single flow event. The observed quadrupolar Eshelby pattern is that predicted from solid-state elasticity theory [46, 62, 65, 68, 80]. Reproduced from Ref. 62.

Lemaitre has worked out the theory for the spatial stress-tensor autocorrelation function in disordered isotropic solids. Remarkably, the $3 \times 3 \times 3 \times 3$ tensor $\langle \sigma_{\alpha\beta}(\mathbf{r}) \sigma_{\gamma\delta}(\mathbf{r}') \rangle$ is determined by just two functions of $|\mathbf{r} - \mathbf{r}'|$ [62, 68]. In general, if X are space or space-time coordinates and D_X a linear differential operator of some field theory with equation of motion "$D_X \phi(X) =$ Noise", one has $D_{X'} \langle \phi(X) \phi(X') \rangle = 0$ whenever X' differs from X in all coordinates. Thus according to the *solid-that-flows* picture, as a function of $\mathbf{r}'$ the autocorrelation function $\langle \sigma_{\alpha\beta}(\mathbf{r}) \sigma_{\gamma\delta}(\mathbf{r}') \rangle$ obeys Eq. (7). In particular, it conforms to the Eshelby theory [80] for $|\mathbf{r} - \mathbf{r}'| \to \infty$. Inci-

dentally, the same must apply for the $\langle \sigma_{\alpha\beta}(\mathbf{r},t)\sigma_{\gamma\delta}(\mathbf{r}',t')\rangle$ for which a theory, however, remains to be found.

Long-ranged stress and strain correlations are only expected below the solidity length. At longer length scales the effects of one flow event are "washed away" by those of others (Sec. II D). Thus beyond the solidity length l_s, an exponential decay of the spatial stress autocorrelation function is expected. This means that in the liquid phase, the Lemaitre spatial autocorrelation functions [68] are to be multiplied by a factor $\sim \exp(-|\mathbf{r}-\mathbf{r}'|/l_s)$.

We finally note that stresses will modify the flow-event energy barriers. This fact is usually not taken into account in attempts to identify likely positions of liquid flow events from locally ordered structures [97], and this may explain why these have only been moderately successful.

IV. EXPERIMENTAL CONSEQUENCES OF SOLIDITY

This section gives three examples of how the *solid-that-flows* viewpoint may elucidate experimental facts of glass-forming liquids. The arguments given all refer to what happens below the solidity length and are based more on intuitive reasoning than on rigorous derivation. The three subsections each deal with points on which there is no general consensus, and the general *solid-that-flows* picture is not invalidated if one or more turn out to be misconceived.

An important discovery of the 1990s was that the dynamics of a glass-forming liquid is spatially inhomogeneous [42, 43, 117–119] in the sense that, at any given time, there are regions of considerable molecular motion and regions of little [22, 120]. This also provides a simple explanation of the observed violation of the Stokes-Einstein relation between viscosity and diffusion coefficient [41, 43, 121]: Fast particles take advantage of rapidly relaxing regions and contribute a lot to $D_{\rm par}$, but little to the overall structural relaxation rate as quantified by τ_α.

What controls the temperature dependence of τ_α? Figure 6(a) presents two fundamentally different scenarios [122]. In one case (upper figure), the local energy barriers control the dynamics in the sense that it basically determines the overall relaxation rate. Alternatively, structural relaxation is considered a highly cooperative process that involves an entire sequence of flow events (lower figure), each of which may not be very large. The latter scenario has been used to explain dynamic heterogeneities and is expected, e.g., from the random first-order transition (RFOT) theory [74, 123]. RFOT is inspired by the theory of spin glasses, which are systems with no elastic interactions. In RFOT the increase of the activation energy of τ_α upon cooling results from a correlation length ξ that grows due to the decrease of entropy [52, 55]. The fundamental RFOT prediction, which has been derived rigorously in infinite dimensions [124], is that thermodynamics control dynamics. For real-life applications, however, this is challenged by the fact that the clever algorithms [125, 126] can speed up computer simulations significantly without affecting the thermodynamics [73, 127].

A. *Dynamic heterogeneity:* Elastic facilitation

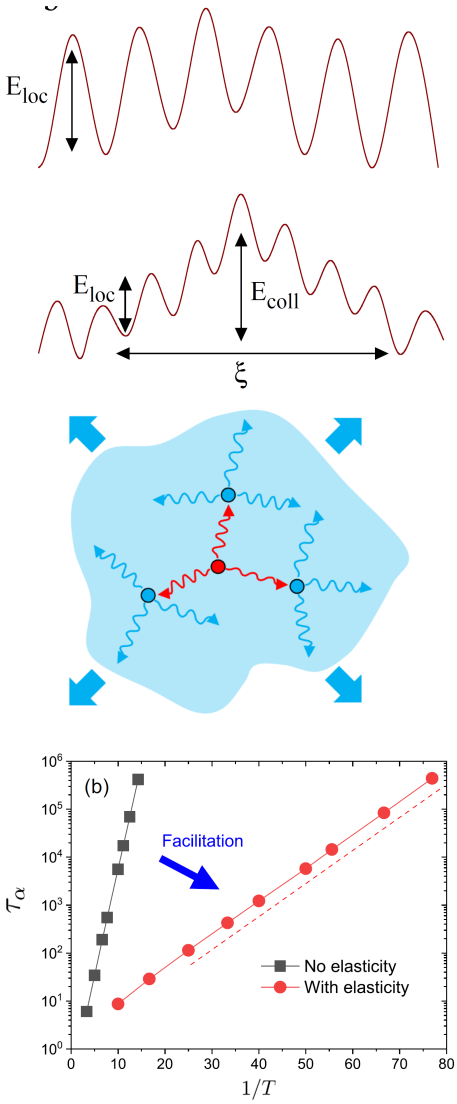

FIG. 6. Elastic facilitation. (a) Schematic free-energy landscape when the dynamics is dominated by local energy barriers (upper figure) or, alternatively, by the growth of cooperative effects over some distance ξ (lower figure). Reproduced from Ref. 122. (b) Avalanche of flow events generated by a single flow event because the induced stress-tensor changes lower some barriers in the surroundings. Reproduced from Ref. 128. (c) Temperature dependence of τ_α in a simple model with and without elastic facilitation. Reproduced from Ref. 129.

The local-barrier picture is the obvious one from the *solid-that-flows* point of view (Sec. IV C) in which the situation is analogous to that of a plastic flow with flow events occurring at soft sites (Sec. III A). That local barriers control the relaxation was demonstrated recently in simulations of a 3d polydisperse soft-repulsive-potential model [122]. By systematically identifying the flow events starting at a given inherent state, it was shown that the activation energy increases and accounts for the super-Arrhenius temperature dependence of τ_α upon cooling. This means that, at least for the model in question, the dynamics is not cooperative; in particular, no divergence of the relaxation time is expected at a finite temperature [125, 130, 131].

If τ_α is controlled by the individual flow-event activation energies, how does one explain dynamic heterogeneity? A promising candidate is facilitation, the general concept that one flow event makes nearby flow events more likely [132–134]. In our case, "elastic facilitation" reflects the fact that any flow event leads to long-ranged stress-tensor changes within the sphere defined by the solidity length, which inevitably lower the barriers of some potential nearby flow events and raise others [47, 62, 129, 135]. The net effect is that one flow event makes neighboring flow events more likely. Elastic facilitation, which was first studied in glasses [62, 136], is illustrated in Fig. 6(b). In a simple model [129], this has been shown to lead to a substantial reduction in the activation energy of τ_α (Fig. 6(c)). In Ref. 128 it was proposed that an entire avalanche of flow events in this way may be triggered by a single one, similar to what happens in plastic flows [87, 137, 138]. Reference 139 considered a simple facilitated trap model [54] and showed that it results in asymmetric loss peaks with an excess wing, somewhat like that of the double-percolation picture we now turn to (see also Refs. 140 and 141).

B. *Non-exponential:* Double-percolation scenario for linear-response functions

Linear response properties are quantified by a complex frequency-dependent response function, $\chi(\omega) = \chi'(\omega) + i\chi''(\omega)$. It is sometimes stated that a major mystery of glass-forming liquids is the observation of broad loss peaks, $\chi''(\omega)$. Certainly, a Debye loss peak, $\chi''(\omega) \propto \omega\tau/[1 + (\omega\tau)^2]$ which according to the fluctuation-dissipation theorem [142] corresponds to an exponential time-autocorrelation function, is rarely observed. But one could also argue that the loss peaks are, in fact, surprisingly *narrow*. In particular, dielectric, mechanical, and specific-heat loss peaks in the vast majority of glass-forming liquids follow the Debye prediction on the low-frequency side. This striking fact implies the existence of a quite sharp long-time cut-off in the relaxation-time distribution $p(\tau)$ defined by formally writing $\chi''(\omega) = \int_0^\infty \omega\tau/[1 + (\omega\tau)^2]p(\tau)d\tau$. How can one understand this?

The disorder of a glass-forming liquid implies that flow-event energy barriers ΔE vary throughout the system. An *ad hoc* assumption is that at any given time the barriers vary randomly in space according to some distribution. This is illustrated in the upper part of Fig. 7(a) for the extreme case of a very wide, flat distribution. Over any brief time interval, the small barriers give rise to what Johari long time ago termed "islands of mobility" [143] in which spatially isolated rearrangements take place. Such islands may involve just a few molecules or be larger and do not necessarily have a well-defined contrast to the surroundings. On a longer time scale flow events involving larger barriers are gradually activated, which at some point percolate the structure. On this time scale extended motion becomes possible within the rigid structure formed by the remaining system. In three dimensions the percolation threshold is roughly one quarter; in two dimensions the threshold is 50% because a given set or its complement must percolate – and for geometric reasons both cannot happen.

Consider next the largest barriers. Being also spatially isolated, these form "islands of immobility". Including gradually smaller barriers, at some point there is "slow-domain percolation", which defines a characteristic time scale that we identify with τ_α: On time scales shorter than τ_α the system is rigid and can sustain an externally imposed shear stress, while on longer time scales than τ_α the slow-domain percolation cluster "dissolves" in a self-reinforcing way, allowing the system to flow in response to an external stress [4]. Single-particle motion is thus predicted to be spatially heterogeneous on short time scales, but homogeneous on time scales longer than τ_α [119, 144–147]. Borrowing a phrase from NMR theory, this has been referred to as "rate exchange" [42, 121, 148]. The result is that the largest barriers are never transcended because they "prefer" to wait until being lowered by elastic facilitation and/or by the collective structural relaxation (flow) taking place on the τ_α time scale. That structural relaxation and thereby τ_α is controlled by the slow particles is an old idea [119, 149–151], which has recently been confirmed in experiments [152], as well as in equilibrium [153, 154] and aging [155] simulations.

The above physical picture translates into a generic frequency-dependent loss, $\chi''(\omega)$, as follows. The largest barriers are never overcome so the corresponding long relaxation times do not contribute to the loss. Consequently, the relaxation-time distribution function $p(\tau)$ has a long-time cutoff roughly at τ_α, and $\chi''(\omega)$ is Debye-like at low frequencies: $\chi''(\omega) \propto \omega$ whenever $\omega\tau_\alpha \ll 1$ [154]. On shorter time scales, i.e., above the α loss-peak frequency, solidity comes into effect resulting in an asymmetric loss peak [153]. Here we predict $\chi''(\omega) \propto \omega^{-1/2}$, which is based on solving a simple field theory for the density fluctuations in the Gaussian approximation, assuming a wavevector-dependent density decay rate of the form $\Gamma(k) = \Gamma_0 + D_{\rm coh}k^2$ in which $\Gamma_0 \sim 1/\tau_\alpha \ll D_{\rm coh}/a^2$ [156]. Conservation laws generally imply a $\Gamma(k) \propto k^2$ type dispersion relation arising from from the spatial

Fourier transform of the ∇^2 operator of the diffusion equation [33, 78]; thus $\Gamma_0 \neq 0$ corresponds to the apparent violation of density conservation discussed in Sec. II E [156]. Note that the picture of Fig. 7(a) corresponds to the extreme case of a wide barrier distribution, which for many equilibrium-liquid systems may be approached only at unreachably low temperatures.

A second loss peak is expected at the frequency corresponding to fast-domain percolation (Fig. 7(a)). Following Gao *et al.* [157] we identify this with the ubiquitous Johari-Goldstein (JG) β process [143], thereby taking several previous works to their logical consequence [158–169].

A double-percolation picture as the above was proposed already in 1996 by Novikov *et al.*, who discussed percolation of liquid-like and solid-like domains defined by, respectively, the largest and smallest vibrational mean-square displacement [170]. A graphic description refers to the slow-domain percolation cluster as a "sponge" through which fast motion is possible [171].

The experimental situation is much less clear than the schematic picture of Fig. 7(a). Thus there are only few data for JG β relaxation in the equilibrium liquid phase. This is because above T_g the α and β processes usually interfere, often to the extent that the high-frequency α decay hides the β process, which is thereby reduced to an excess wing of the α process [153, 172, 173]. Turning now to the α process, an analysis of more than 300 dielectric spectra revealed that the α high-frequency approximate exponent – identified as the minimum slope in a log-log plot, $\alpha_{\min}$ – is predominantly found to be close to -0.5 (Fig. 7(b)); $\alpha_{\min}$ moreover appears to approach -0.5 as $T \to T_g$ [174]. Recent light-scattering data confirm this picture [175, 176], compare Fig. 7(c); we also note that recent extensive computer simulations find an exponent of -0.38 [154], which is not far from -0.5.

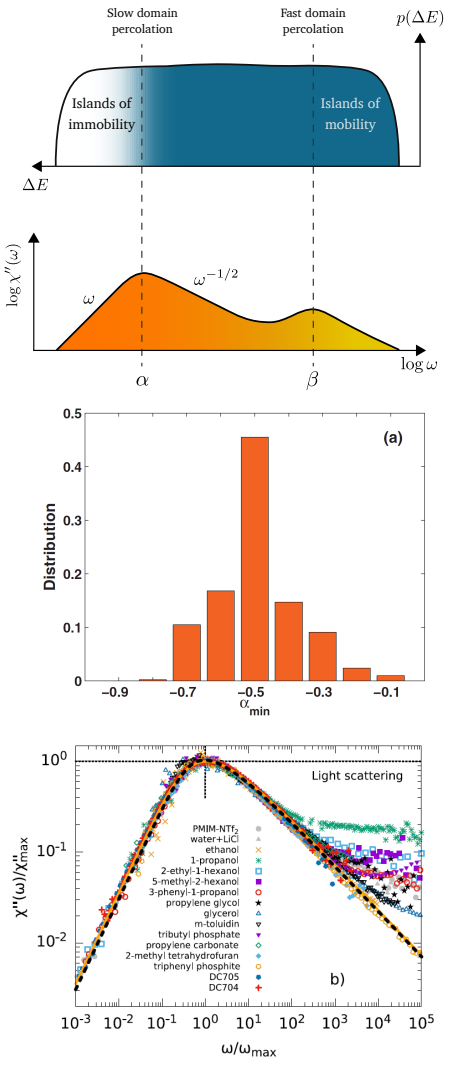

FIG. 7. Linear-response consequences of glass-forming liquids' solidity. (a) Schematic picture of the double-percolation scenario proposed to control linear-response properties for the case of a very broad activation-energy distribution. The distribution is constant in time, but the activation energy of any single region changes over the τ_α time scale. The islands of immobility do not contribute to any relaxation because their barriers are too high and await being lowered by elastic facilitation and/or the dissolving of the entire slow-domain percolation cluster on the τ_α time scale. (b) Minimum-slope histogram of log-log dielectric losses for 347 spectra at different temperatures of 53 liquids. The prevalent minimum slopes are close to -0.5. Reproduced from Ref. 174. (c) Results from dynamic light scattering showing a $\chi''(\omega) \propto \omega^{-1/2}$ high-frequency decay. The black dashed line is the imaginary part of $\chi(\omega) \propto 1/\sqrt{1+i\omega\tau_\alpha} + 1/(\sqrt{2}+\sqrt{1+i\omega\tau_\alpha})$, which has been derived from the density-dispersion relation $\Gamma(k) = \Gamma_0 + D_{\rm coh}k^2$ that incorporates the apparent violation of density conservation (Sec. II E) [184]. Reproduced from Ref. 175.

C. *Non-Arrhenius:* Elastic models for the temperature dependence of τ_α

Point defects in simple crystals are either vacancies or interstitials, i.e., missing or extra atoms [69, 177]. Such defects can jump, and the activation energy for a jump scales with the crystal's elastic constants [178]. In the *solid-that-flows* picture it is obvious to assume that the flow-event activation energy likewise is proportional to the elastic constants, here those that characterize fast deformations of the surrounding medium, i.e., the high-frequency plateau shear and bulk moduli. This idea defines the elastic models that exist in several versions [11, 179] and have been linked to models based on decrease of free volume or growth of collective motion upon cooling [147, 180]. In some models [181–183] elasticity accounts for only part of the activation energy, however.

Just as for a plastic flow (Sec. III A), flow events in a glass-forming liquid preferably take place at soft spots

[185, 186] (Fig. 4(b)). The simplest mean-field approach ignores this and assumes that all flow-event activation energies scale in proportion to the macroscopic moduli. For a perfectly spherical flow event in a homogeneous material, the surroundings experience as mentioned a radial displacement $\propto 1/r^2$. This results in a pure shear deformation, i.e., with no density change (Sec. II C). Thus the relevant elastic constant is the high-frequency plateau shear modulus G_∞ that – ignoring the existence of dynamic heterogeneities – defines the shoving model according to which [187]

$$\tau_\alpha \;=\; \tau_0\, e^{G_\infty(T) V_c / k_B T}\,. \tag{8}$$

Here $\tau_0 \sim 10^{-13}$s is a prefactor set by the phonon time scale and V_c is a microscopic volume. G_∞ of a glass-forming liquid is usually much more temperature dependent than in the corresponding crystal; in fact $G_\infty(T)$ often increases upon cooling enough to fully account for the non-Arrhenius $\tau_\alpha(T)$. The physical picture of the shoving model is given in Fig. 4(a), but many data conform to Eq. (8) [183]; an example of this is given in Fig. 8(b). Equation (8) does not apply for all glass-forming liquids, though [183, 188].

In so far as the dominant contribution to the activation energy derives from displacements around the flow event and not at its center, G_∞ controls more than 90% of the activation energy [189]. Elastic models emphasizing instead the bulk modulus also exist, however [183, 190]. A popular elastic model expression is $\log(\tau_\alpha) \propto 1/\langle u^2\rangle$ in which $\langle u^2\rangle$ is the vibrational mean-square displacement [11, 183, 191–194]. In this approach T_g is characterized by a definite value of $1/\langle u^2\rangle$, which gives rise to a glass version of the Lindemann melting criterion [195–197]. This prediction has been investigated for metallic glasses by taking V_c to be a fixed fraction of the molar volume V_m and assuming that all vibrations are phonons controlled by G_∞ and the high-frequency plateau bulk modulus, K_∞. At the glass transition these moduli freeze into their glass values, G and K, which leads to the prediction [198]

$$T_g \propto G\, V_m \frac{K + 4G/3}{2K + 11G/3} \tag{9}$$

with a universal constant of proportionality. This is validated in Fig. 8(c), thus connecting glass properties to the liquid dynamics [199].

The above approaches either assume that the elastic properties are constant throughout the sample or that all local elastic constants [200, 201] scale proportionally when temperature is changed [202]. Kapteijns *et al.* studied the energy landscape of a binary Lennard-Jones model to investigate the influence of the pairwise elastic constants on the temperature dependence of τ_α [203]. The activation energy of τ_α was found to be proportional to the average "stiffness" between neighboring particles of the liquid's inherent structures. This leads to the straight-line prediction of Fig. 8(d) that suggests a microscopic explanation of why elastic models account for many non-Arrhenius data [188].

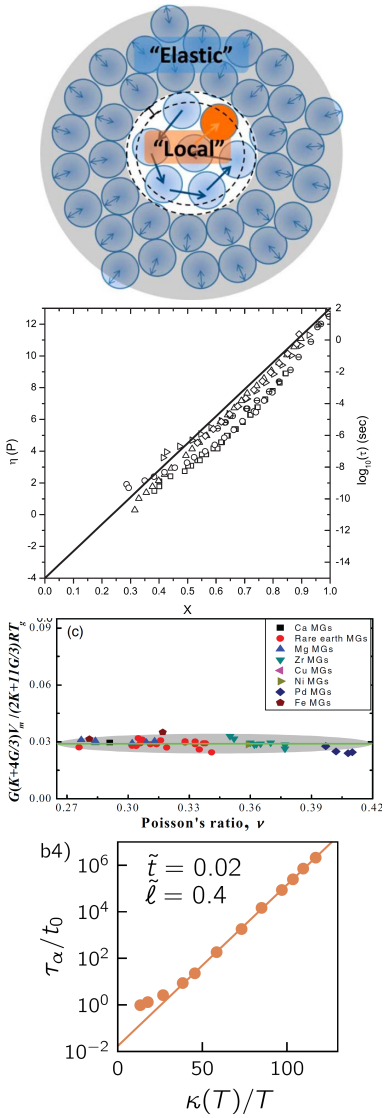

FIG. 8. (a) Schematic picture of a flow event. The shoving model ignores the "local" contribution to the activation energy [204, 205]. Reproduced from Ref. 205. (b) Log(viscosity) of ten organic glass-forming liquids plotted as a function of $X \equiv G_\infty(T)T_g/(G_\infty(T_g)T)$. Equation (8) predicts a straight line ending at the high-temperature viscosity (10^{-4} Poise = 10^{-5} Pa·s). Reproduced from Ref. 206. (c) Test of Eq. (9) for metallic glasses in which G and K are the glass shear and bulk moduli and V_m the molar volume. There are no free parameters. Reproduced from Ref. 198. (d) For a binary Lennard-Jones model the activation energy of τ_α is proportional to the average microscopic dipole stiffness κ, leading to the prediction $\log(\tau_\alpha/t_0) \propto \kappa(T)/T$ in which t_0 is phonon time. Reproduced from Ref. 203.

V. DISCUSSION

This paper has reviewed arguments that a glass-forming liquid below the solidity length is more like a *solid-that-flows* than like "ordinary" less viscous liquids. The focus has been on the dynamics, leaving out a discussion of thermodynamic properties and their correlation to the dynamics [17, 52]. In regard to possible experimental consequences, we note that the double-percolation picture does not apply in 2d. That is, if α and β relaxations as suggested derive from slow- and fast-domain percolation, respectively, no separate (Johari-Goldstein) β relaxation should exist in 2d because the percolation threshold is here 50%. Interestingly, it has been argued from simulations that the glass transition in 2d indeed is different from in 3d in several respects [125, 207, 208]. Another prediction of the above is that all molecules contribute to the β relaxation in the liquid phase, albeit only a fraction of them at any given time, while in the glass some molecules contribute and some do not [154, 209].

Not everything discussed in this paper can be correct for the simple reason that there are several inconsistencies. We end the paper by listing these and other issues in order to illustrate that there is still no self-contained picture of glass-forming liquids' solidity and its consequences:

- The derivation of the solidity length Eq. (4) assumes that each place in the liquid on average gives rise to one flow event every τ_α. This is inconsistent with the double-percolation picture of Fig. 7(a) in which a broad range of activation energies is involved. This inconsistency persists even after taking into account that the "islands of immobility" are renormalized and lowered to the "percolation" activation energy of τ_α. This dilemma may be resolved by following Furukawa and instead define l_s as the length scale beyond which ordinary hydrodynamics applies [75]; as noted in Sec. II D this leads to virtually the same expression as Eq. (4). Incidentally, while $l_\mathrm{s} \propto \tau_\alpha^{1/4}$ has recently been confirmed in connection with nonlinear flow modeling [210], other recent works predict $l_\mathrm{s} \propto \tau_\alpha^{1/2}$ [211] and $l_\mathrm{s} \propto \tau_\alpha^{1/3}$ [5], a matter that needs to be clarified. How to determine l_s in experiments is another important challenge for future work [210].

- The coarse-grained description of the apparent violation of particle number conservation, Eq. (6), is based on spherically symmetric flow events. In reality the flow-event force quadrupole moment is usually non-zero [62, 65, 80], leading to minor long-ranged density changes. Moreover, even for a hypothetical perfectly spherical flow event, there will be minor "advective" density changes because the density varies slightly in space. Both types of density changes sum to zero, however, and do not lead to a coarse-grained density-conserving dynamics.

- It is not obvious that elastic facilitation (Fig. 6(b) and (c)) is enough to eradicate the largest quarter of the local energy barriers (Fig. 7(a)). After all, the stress changes of one flow event decays in space as $\propto 1/r^3$, which is rather rapid so other facilitation mechanisms may be needed [154, 212]. We favor the above-mentioned possibility that the whole system flows on time scales longer than τ_α on which all stresses are relaxed, including those that keep in place the solid structure defining the energy barriers.

- Based on the double-percolation picture one would expect an experimental signature of the percolation critical exponents [153, 213], which contradicts the prediction that $\chi''(\omega) \propto \omega^{-1/2}$ above the α loss peak frequency. Moreover, it was recently shown that the (zero-parameter) random-barrier model provides an excellent fit to the inherent mean-square displacement as a function of time for a binary ultraviscous Lennard-Jones liquid [214]. It is not obvious how to reconcile that model [215] with the prediction for the α high-frequency loss, $\chi''(\omega) \propto \omega^{-1/2}$.

- The shoving model assumes uniform elasticity on the short time scale. If one assumes that all flow-event barriers scale in proportion when temperature is changed, this temperature scaling is inherited by $G_\infty(T)$ [202]. Even under this assumption, however, one would expect the flow-event sequences not to be temperature invariant because sequences avoiding large barriers will be increasingly important as the temperature is lowered.

Clearly, much further work is needed before the *solid-that-flows* picture has matured into a simple and coherent one.

ACKNOWLEDGMENTS

This work was supported by the VILLUM Foundation's *Matter* grant (VIL16515).

[1] J. L. Lebowitz, Statistical mechanics – A review of selected rigorous results, Annu. Rev. Phys. Chem. **19**, 389 (1968).

[2] F. Sausset, G. Biroli, and J. Kurchan, Do solids flow?, J. Stat. Phys. **140**, 718 (2010).

[3] S. Saw and P. Harrowell, Rigidity in condensed matter and its origin in configurational constraint, Phys. Rev. Lett. **116**, 137801 (2016).

[4] H. Tong, S. Sengupta, and H. Tanaka, Emergent solidity of amorphous materials as a consequence of mechanical self-organisation, Nat. Commun. **11**, 4863 (2020).

[5] A. Furukawa, Transverse viscous transport in classical solid states, Phys. Rev. Lett. **127**, 245901 (2021).

[6] M. Baggioli, M. Landry, and A. Zaccone, Deformations, relaxation, and broken symmetries in liquids, solids, and glasses: A unified topological field theory, Phys. Rev. E **105**, 024602 (2022).

[7] C.-H. Tu, M. Steinhart, R. Berger, M. Kappl, H.-J. Butt, and G. Floudas, When crystals flow, Sci. Adv. **9**, eadg8865 (2023).

[8] G. P. Johari, Introduction to the glassy state in the undergraduate curriculum, J. Chem. Educ. **51**, 23 (1974).

[9] C. A. Angell, Formation of glasses from liquids and biopolymers, Science **267**, 1924 (1995).

[10] P. G. Debenedetti and F. H. Stillinger, Supercooled liquids and the glass transition, Nature **410**, 259 (2001).

[11] J. C. Dyre, The glass transition and elastic models of glass-forming liquids, Rev. Mod. Phys. **78**, 953 (2006).

[12] C. Alba-Simionesco and G. Tarjus, A perspective on the fragility of glass-forming liquids, J. Non-Cryst. Solids X **14**, 100100 (2022).

[13] G. Harrison, *The Dynamic Properties of Supercooled Liquids* (Academic, New York, 1976).

[14] S. Brawer, *Relaxation in Viscous Liquids and Glasses* (American Ceramic Society, Columbus, OH, 1985).

[15] A. K. Varshneya, *Fundamentals of Inorganic Glasses* (Academic, New York, 1994).

[16] M. D. Ediger, C. A. Angell, and S. R. Nagel, Supercooled liquids and glasses, J. Phys. Chem **100**, 13200 (1996).

[17] C. A. Angell, K. L. Ngai, G. B. McKenna, P. F. McMillan, and S. W. Martin, Relaxation in glassforming liquids and amorphous solids, J. Appl. Phys. **88**, 3113 (2000).

[18] L. Berthier and G. Biroli, Theoretical perspective on the glass transition and amorphous materials, Rev. Mod. Phys. **83**, 587 (2011).

[19] G. L. Hunter and E. R. Weeks, The physics of the colloidal glass transition, Rep. Prog. Phys. **75**, 066501 (2012).

[20] W. H. Wang, The elastic properties, elastic models and elastic perspectives of metallic glasses, Prog. Mater. Sci. **57**, 487 (2012).

[21] G. B. McKenna and S. L. Simon, 50th anniversary perspective: Challenges in the dynamics and kinetics of glass-forming polymers, Macromolecules **50**, 6333 (2017).

[22] H. Tanaka, H. Tong, R. Shi, and J. Russo, Revealing key structural features hidden in liquids and glasses, Nat. Rev. Phys. **1**, 333 (2019).

[23] J. C. Mauro, *Materials Kinetics: Transport and Rate Phenomena* (Elsevier, Amsterdan, Netherlands, 2021).

[24] C. Alba-Simionesco, Organic glass-forming liquids and the concept of fragility, C. R. Phys. **24**, 10.5802/crphys.148 (2023).

[25] L. D. Landau and E. M. Lifshitz, *Fluid Mechanics* (Pergamon, Oxford, 1959).

[26] B. Lautrup, *Physics of Continuous Matter*, 2nd ed. (CRC Press, 2011).

[27] E. N. C. Andrade, A theory of the viscosity of liquids. – Part I, The London, Edinburgh, and Dublin Philosophical Magazine and Journal of Science **17**, 497 (1934).

[28] J. Frenkel, *Kinetic Theory of Liquids* (Clarendon, Oxford, 1946).

[29] J. O. Hirschfelder, C. F. Curtiss, and R. B. Bird, *Molecular Theory of Gases and Liquids* (John Wiley & Sons, New York, 1954).

[30] K. Trachenko, *Theory of liquids: From excitations to thermodynamics* (Cambridge University Press, 2023).

[31] M. Mooney, A theory of the viscosity of a Maxwellian elastic liquid, Trans. Soc. Rheol. **1**, 63 (1957).

[32] J. Lamb, Viscoelasticity and lubrication: A review of liquid properties, J. Rheol. **22**, 317 (1978).

[33] J.-P. Hansen and I. R. McDonald, *Theory of Simple Liquids: With Applications to Soft Matter*, 4th ed. (Academic, New York, 2013).

[34] J.-L. Barrat and J.-P. Hansen, *Basic Concepts for Simple and Complex Liquids* (Cambridge University Press, 2003).

[35] A. K. Bacher, T. B. Schrøder, and J. C. Dyre, Explaining why simple liquids are quasi-universal, Nat. Commun. **5**, 5424 (2014).

[36] J. C. Dyre, Simple liquids' quasiuniversality and the hard-sphere paradigm, J. Phys. Condens. Matter **28**, 323001 (2016).

[37] A. K. Bacher, T. B. Schrøder, and J. C. Dyre, The EXP pair-potential system. I. Fluid phase isotherms, isochores, and quasiuniversality, J. Chem. Phys. **149**, 114501 (2018).

[38] L. Costigliola, D. M. Heyes, T. B. Schrøder, and J. C. Dyre, Revisiting the Stokes-Einstein relation without a hydrodynamic diameter, J. Chem. Phys. **150**, 021101 (2019).

[39] J. S. Hansen, *Nanoscale Hydrodynamics of Simple Systems* (Cambridge University Press, 2022).

[40] F. Fujara, B. Geil, H. Sillescu, and G. Fleischer, Translational and rotational diffusion in supercooled orthoterphenyl close to the glass transition, Z. Phys. B – Cond. Mat. **88**, 195 (1992).

[41] G. Tarjus and D. Kivelson, Breakdown of the Stokes–Einstein relation in supercooled liquids, J. Chem. Phys. **103**, 3071 (1995).

[42] H. Sillescu, Heterogeneity at the glass transition: a review, J. Non-Cryst. Solids **243**, 81 (1999).

[43] M. D. Ediger, Spatially heterogeneous dynamics in supercooled liquids, Annu. Rev. Phys. Chem. **51**, 99 (2000).

[44] K. R. Harris, The fractional Stokes–Einstein equation: Application to Lennard-Jones, molecular, and ionic liquids, J. Chem. Phys. **131**, 054503 (2009).

[45] B. E. Poling, J. M. Prausnitz, and J. P. O'Connell, *The properties of Gases and Liquids*, 5th ed. (McGraw-Hill, New York, 2001).

[46] L. D. Landau and E. M. Lifshitz, *Theory of Elasticity* (Pergamon, Oxford, 1959).

[47] R. N. Chacko, F. P. Landes, G. Biroli, O. Dauchot, A. J. Liu, and D. R. Reichman, Elastoplasticity mediates dynamical heterogeneity below the mode coupling temperature, Phys. Rev. Lett. **127**, 048002 (2021).

[48] J. P. Stoppelman, J. G. McDaniel, and M. T. Cicerone, Excitations follow (or lead?) density scaling in propy-

lene carbonate, J. Chem. Phys. **157**, 204506 (2022).
[49] W. H. Wang, Dynamic relaxations and relaxation-property relationships in metallic glasses, Prog. Mater. Sci. **106**, 100561 (2019).
[50] T. B. Schrøder, S. Sastry, J. C. Dyre, and S. C. Glotzer, Crossover to potential energy landscape dominated dynamics in a model glass-forming liquid, J. Chem. Phys. **112**, 9834 (2000).
[51] W. Kauzmann, The nature of the glassy state and the behavior of liquids at low temperatures, Chem. Rev. **43**, 219 (1948).
[52] G. Adam and J. H. Gibbs, On temperature dependence of cooperative relaxation properties in glass-forming liquids, J. Chem. Phys. **43**, 139 (1965).
[53] M. Goldstein, Glass and other relaxations in liquids, Faraday Symp. Chem. Soc. **6**, 7 (1972).
[54] J. C. Dyre, Master-equation approach to the glass transition, Phys. Rev. Lett. **58**, 792 (1987).
[55] V. Lubchenko and P. G. Wolynes, Theory of Structural Glasses and Supercooled Liquids, Annu. Rev. Phys. Chem. **58**, 235 (2007).
[56] S. Mirigian and K. S. Schweizer, Elastically cooperative activated barrier hopping theory of relaxation in viscous fluids. II. Thermal liquids., J. Chem. Phys. **140**, 194507 (2014).
[57] Z. Wang and W.-H. Wang, Flow units as dynamic defects in metallic glassy materials, Natl. Sci. Rev. **6**, 304 (2019).
[58] M. Goldstein, Viscous liquids and the glass transition: A potential energy barrier picture, J. Chem. Phys. **51**, 3728 (1969).
[59] F. H. Stillinger, A topographic view of supercooled liquids and glass formation, Science **267**, 1935 (1995).
[60] B. Doliwa and A. Heuer, What does the potential energy landscape tell us about the dynamics of supercooled liquids and glasses?, Phys. Rev. Lett. **91**, 235501 (2003).
[61] J. Chattoraj and A. Lemaitre, Elastic signature of flow events in supercooled liquids under shear, Phys. Rev. Lett. **111**, 066001 (2013).
[62] A. Lemaitre, Structural relaxation is a scale-free process, Phys. Rev. Lett. **113**, 245702 (2014).
[63] B. Illing, S. Fritschi, D. Hajnal, C. Klix, P. Keim, and M. Fuchs, Strain pattern in supercooled liquids, Phys. Rev. Lett. **117**, 208002 (2016).
[64] R. Böhmer and G. Hinze, Reorientations in supercooled glycerol studied by two-dimensional time-domain deuteron nuclear magnetic resonance spectroscopy, J. Chem. Phys. **109**, 241 (1998).
[65] J. D. Eshelby, The determination of the elastic field of an ellipsoidal inclusion, and related problems, Proc. Roy. Soc. (London) **241**, 376 (1957).
[66] J. C. Dyre, Solidity of viscous liquids. II. Anisotropic flow events, Phys. Rev. E **59**, 7243 (1999).
[67] A. Lemaitre, Tensorial analysis of Eshelby stresses in 3D supercooled liquids, J. Chem. Phys. **143**, 164515 (2015).
[68] A. Lemaitre, Stress correlations in glasses, J. Chem. Phys. **149**, 104107 (2018).
[69] N. W. Ashcroft and N. D. Mermin, *Solid State Physics* (Holt, Rinehart and Winston, 1976).
[70] J. C. Dyre, Solidity of viscous liquids, Phys. Rev. E **59**, 2458 (1999).
[71] L. Berthier, G. Biroli, J.-P. Bouchaud, L. Cipelletti, and W. van Saarloos, eds., *Dynamical Heterogeneities in Glasses, Colloids, and Granular Media* (Oxford Univ. Press, 2011).
[72] S. Karmakar, C. Dasgupta, and S. Sastry, Growing length scales and their relation to timescales in glass-forming liquids, Annu. Rev. Cond. Mat. Phys. **5**, 255 (2014).
[73] M. Wyart and M. E. Cates, Does a growing static length scale control the glass transition?, Phys. Rev. Lett. **119**, 195501 (2017).
[74] G. Biroli and J. P. Bouchaud, The RFOT theory of glasses: Recent progress and open issues, C. R. Phys. **24**, 10.5802/crphys.136 (2023).
[75] A. Furukawa, Simple picture of supercooled liquid dynamics: Dynamic scaling and phenomenology based on clusters, Phys. Rev. E **87**, 062321 (2013).
[76] A. Furukawa, The emergence of cooperativity accompanying vitrification: insights from density fluctuation dynamics, J. Stat. Mech. **2019**, 084001 (2019).
[77] T. Hecksher, N. B. Olsen, K. A. Nelson, J. C. Dyre, and T. Christensen, Mechanical spectra of glass-forming liquids. I. Low-frequency bulk and shear moduli of DC704 and 5-PPE measured by piezoceramic transducers, J. Chem. Phys. **138**, 12A543 (2013).
[78] L. P. Kadanoff and P. C. Martin, Hydrodynamic equations and correlation functions, Ann. Phys. **24**, 419 (1963).
[79] P. C. Martin, O. Parodi, and P. S. Pershan, Unified hydrodynamic theory for crystals, liquid crystals, and normal fluids, Phys. Rev. A **6**, 2401 (1972).
[80] J. D. Eshelby, The elastic field outside an ellipsoidal inclusion, Proc. Roy. Soc. (London) **252**, 561 (1959).
[81] A. Barbot, M. Lerbinger, A. Hernandez-Garcia, R. Garcia-Garcia, M. L. Falk, D. Vandembroucq, and S. Patinet, Local yield stress statistics in model amorphous solids, Phys. Rev. E **97**, 033001 (2018).
[82] M. Lerbinger, A. Barbot, D. Vandembroucq, and S. Patinet, Relevance of shear transformations in the relaxation of supercooled liquids, Phys. Rev. Lett. **129**, 195501 (2022).
[83] P. Schall, D. A. Weitz, and F. Spaepen, Structural rearrangements that govern flow in colloidal glasses, Science **318**, 1895 (2007).
[84] J. Lin, E. Lerner, A. Rosso, and M. Wyart, Scaling description of the yielding transition in soft amorphous solids at zero temperature, PNAS **111**, 14382 (2014).
[85] T. Voigtmann, Nonlinear glassy rheology, Curr. Opin. Colloid Interface Sci. **19**, 549 (2014).
[86] T. C. Hufnagel, C. A. Schuh, and M. L. Falk, Deformation of metallic glasses: Recent developments in theory, simulations, and experiments, Acta Materialia **109**, 375 (2016).
[87] A. Nicolas, E. E. Ferrero, K. Martens, and J.-L. Barrat, Deformation and flow of amorphous solids: Insights from elastoplastic models, Rev. Mod. Phys. **90**, 045006 (2018).
[88] D. Richard, M. Ozawa, S. Patinet, E. Stanifer, B. Shang, S. A. Ridout, B. Xu, G. Zhang, P. K. Morse, J.-L. Barrat, L. Berthier, M. L. Falk, P. Guan, A. J. Liu, K. Martens, S. Sastry, D. Vandembroucq, E. Lerner, and M. L. Manning, Predicting plasticity in disordered solids from structural indicators, Phys. Rev. Mater. **4**, 113609 (2020).
[89] M. L. Falk and J. S. Langer, Dynamics of viscoplastic deformation in amorphous solids, Phys. Rev. E **57**, 7192 (1998).

[90] A. Tanguy, F. Leonforte, and J.-L. Barrat, Plastic response of a 2D Lennard-Jones amorphous solid: Detailed analysis of the local rearrangements at very slow strain rate, Eur. Phys. J. E **20**, 355 (2006).

[91] E. Bouchbinder, J. S. Langer, and I. Procaccia, Athermal shear-transformation-zone theory of amorphous plastic deformation. I. Basic principles, Phys. Rev. E **75**, 036107 (2007).

[92] E. Lerner, Micromechanics of nonlinear plastic modes, Phys. Rev. E **93**, 053004 (2016).

[93] A. Widmer-Cooper and P. Harrowell, Predicting the long-time dynamic heterogeneity in a supercooled liquid on the basis of short-time heterogeneities, Phys. Rev. Lett. **96**, 185701 (2006).

[94] J. Zylberg, E. Lerner, Y. Bar-Sinai, and E. Bouchbinder, Local thermal energy as a structural indicator in glasses, PNAS **114**, 7289 (2017).

[95] S. Patinet, D. Vandembroucq, and M. L. Falk, Connecting local yield stresses with plastic activity in amorphous solids, Phys. Rev. Lett. **117**, 045501 (2016).

[96] D. Coslovich, Locally preferred structures and many-body static correlations in viscous liquids, Phys. Rev. E **83**, 051505 (2011).

[97] C. P. Royall and S. R. Williams, The role of local structure in dynamical arrest, Physics Reports **560**, 1 (2015).

[98] M. K. Nandi and S. M. Bhattacharyya, Microscopic theory of softness in supercooled liquids, Phys. Rev. Lett. **126**, 208001 (2021).

[99] E. D. Cubuk, R. J. S. Ivancic, S. S. Schoenholz, D. J. Strickland, A. Basu, Z. S. Davidson, J. Fontaine, J. L. Hor, Y.-R. Huang, Y. Jiang, N. C. Keim, K. D. Koshigan, J. A. Lefever, T. Liu, X.-G. Ma, D. J. Magagnosc, E. Morrow, C. P. Ortiz, J. M. Rieser, A. Shavit, T. Still, Y. Xu, Y. Zhang, K. N. Nordstrom, P. E. Arratia, R. W. Carpick, D. J. Durian, Z. Fakhraai, D. J. Jerolmack, D. Lee, J. Li, R. Riggleman, K. T. Turner, A. G. Yodh, D. S. Gianola, and A. J. Liu, Structure-property relationships from universal signatures of plasticity in disordered solids, Science **358**, 1033 (2017).

[100] E. Boattini, S. Marín-Aguilar, S. Mitra, G. Foffi, F. Smallenburg, and L. Filion, Autonomously revealing hidden local structures in supercooled liquids, Nat. Commun. **11**, 5479 (2020).

[101] A. Widmer-Cooper, H. Perry, P. Harrowell, and D. R. Reichman, Irreversible reorganization in a supercooled liquid originates from localized soft modes, Nat. Phys. **4**, 711 (2008).

[102] A. Tanguy, B. Mantisi, and M. Tsamados, Vibrational modes as a predictor for plasticity in a model glass, Europhys. Lett. **90**, 16004 (2010).

[103] M. L. Manning and A. J. Liu, Vibrational modes identify soft spots in a sheared disordered packing, Phys. Rev. Lett. **107**, 108302 (2011).

[104] E. Lerner and E. Bouchbinder, Low-energy quasilocalized excitations in structural glasses, J. Chem. Phys. **155**, 200901 (2021).

[105] Z. W. Wu, Y. Chen, W.-H. Wang, W. Kob, and L. Xu, Topology of vibrational modes predicts plastic events in glasses, Nat. Commun. **14**, 2955 (2023).

[106] G. Kapteijns, D. Richard, and E. Lerner, Nonlinear quasilocalized excitations in glasses: True representatives of soft spots, Phys. Rev. E **101**, 032130 (2020).

[107] G. Picard, A. Ajdari, F. Lequeux, and L. Bocquet, Elastic consequences of a single plastic event: A step towards the microscopic modeling of the flow of yield stress fluids, Eur. J. Phys. E **15**, 371 (2004).

[108] V. Chikkadi, G. Wegdam, D. Bonn, B. Nienhuis, and P. Schall, Long-range strain correlations in sheared colloidal glasses, Phys. Rev. Lett. **107**, 198303 (2011).

[109] S. Chowdhury, S. Abraham, T. Hudson, and P. Harrowell, Long range stress correlations in the inherent structures of liquids at rest, J. Chem. Phys. **144**, 124508 (2016).

[110] U. Buchenau, Eshelby description of highly viscous flow – Half model, half theory, J. Chem. Phys. **149**, 044508 (2018).

[111] M. R. Hasyim and K. K. Mandadapu, A theory of localized excitations in supercooled liquids, J. Chem. Phys. **155**, 044504 (2021).

[112] Y.-W. Li, Y. Yao, and M. P. Ciamarra, Local plastic response and slow heterogeneous dynamics of supercooled liquids, Phys. Rev. Lett. **128**, 258001 (2022).

[113] E. Flenner and G. Szamel, Long-range spatial correlations of particle displacements and the emergence of elasticity, Phys. Rev. Lett. **114**, 025501 (2015).

[114] M. Maier, A. Zippelius, and M. Fuchs, Emergence of long-ranged stress correlations at the liquid to glass transition, Phys. Rev. Lett. **119**, 265701 (2017).

[115] L. Klochko, J. Baschnagel, J. P. Wittmer, H. Meyer, O. Benzerara, and A. N. Semenov, Theory of length-scale dependent relaxation moduli and stress fluctuations in glass-forming and viscoelastic liquids, J. Chem. Phys. **156**, 164505 (2022).

[116] D. Steffen, L. Schneider, M. Müller, and J. Rottler, Molecular simulations and hydrodynamic theory of nonlocal shear-stress correlations in supercooled fluids, J. Chem. Phys. **157**, 064501 (2022).

[117] M. M. Hurley and P. Harrowell, Kinetic structure of a two-dimensional liquid, Phys. Rev. E **52**, 1694 (1995).

[118] B. Schiener, R. Böhmer, A. Loidl, and R. V. Chamberlin, Nonresonant spectral hole burning in the slow dielectric response of supercooled liquids, Science **274**, 752 (1996).

[119] S. C. Glotzer, Spatially heterogeneous dynamics in liquids: insights from simulation, J. Non-Cryst. Solids **274**, 342 (2000).

[120] L. Berthier, Self-induced heterogeneity in deeply supercooled liquids, Phys. Rev. Lett. **127**, 088002 (2021).

[121] G. Diezemann, A free-energy landscape model for primary relaxation in glass-forming liquids: Rotations and dynamic heterogeneities, J. Chem. Phys. **107**, 10112 (1997).

[122] M. P. Ciamarra, W. Ji, and M. Wyart, Local barriers control relaxation near the glass transition up to millisecond time scales, arXiv , 2302.05150 (2023).

[123] P. G. Wolynes and V. Lubchenko, *Structural Glasses and Supercooled Liquids: Theory, Experiment, and Applications* (Wiley, New York, 2012).

[124] G. Parisi, P. Urbani, and F. Zamponi, *Theory of Simple Glasses* (Cambridge University Press, 2020).

[125] L. Santen and W. Krauth, Absence of thermodynamic phase transition in a model glass former, Nature **405**, 550 (2000).

[126] A. Ninarello, L. Berthier, and D. Coslovich, Models and algorithms for the next generation of glass transition studies, Phys. Rev. X **7**, 021039 (2017).

[127] C. Gavazzoni, C. Brito, and M. Wyart, Testing theories of the glass transition with the same liquid, but many

kinetic rules, , arXiv:2308.00196.
[128] A. Tahaei, G. Biroli, M. Ozawa, M. Popovic, and M. Wyart, Scaling description of dynamical heterogeneity and avalanches of relaxation in glass-forming liquids, Phys. Rev. X **13**, 031034 (2023).
[129] M. Ozawa and G. Biroli, Elasticity, facilitation, and dynamic heterogeneity in glass-forming liquids, Phys. Rev. Lett. **130**, 138201 (2023).
[130] T. Hecksher, A. I. Nielsen, N. B. Olsen, and J. C. Dyre, Little evidence for dynamic divergences in ultraviscous molecular liquids, Nat. Phys. **4**, 737 (2008).
[131] G. B. McKenna and J. Zhao, Accumulating evidence for non-diverging time-scales in glass-forming fluids, J. Non-Cryst. Solids **407**, 3 (2015).
[132] G. H. Fredrickson and H. C. Andersen, Kinetic Ising model of the glass transition, Phys. Rev. Lett. **53**, 1244 (1984).
[133] J. P. Garrahan and D. Chandler, Geometrical explanation and scaling of dynamical heterogeneities in glass forming systems, Phys. Rev. Lett. **89**, 035704 (2002).
[134] F. Ritort and P. Sollich, Glassy dynamics of kinetically constrained models, Adv. Phys. **52**, 219 (2003).
[135] G. Zhang, H. Xiao, E. Yang, J. S. Robert, S. A. Ridout, R. A. Riggleman, D. J. Durian, and A. J. Liu, Structuro-elasto-plasticity model for large deformation of disordered solids, Phys. Rev. Res. **4**, 043026 (2022).
[136] J. Duan, Y. J. Wang, L. H. Dai, and M. Q. Jiang, Elastic interactions of plastic events in strained amorphous solids before yield, Phys. Rev. Mater. **7**, 013601 (2023).
[137] B. Shang, P. Guan, and J.-L. Barrat, Elastic avalanches reveal marginal behavior in amorphous solids, PNAS **117**, 86 (2020).
[138] D. Richard, A. Elgailani, D. Vandembroucq, M. L. Manning, and C. E. Maloney, Mechanical excitation and marginal triggering during avalanches in sheared amorphous solids, Phys. Rev. E **107**, 034902 (2023).
[139] C. Scalliet, B. Guiselin, and L. Berthier, Excess wings and asymmetric relaxation spectra in a facilitated trap model, J. Chem. Phys. **155**, 064505 (2021).
[140] M. R. Hasyim and K. K. Mandadapu, Emergent facilitation and glassy dynamics in supercooled liquids, arXiv:2310.06584 (2023).
[141] S. A. Ridout, I. Tah, and A. J. Liu, Building a "trap model" of glassy dynamics from a local structural predictor of rearrangements, Europhys. Lett. , Accepted manuscript (2023).
[142] L. E. Reichl, *A Modern Course in Statistical Physics*, 4th ed. (Wiley-VCH, 2016).
[143] G. P. Johari and M. Goldstein, Viscous liquids and the glass transition. II. Secondary relaxations in glasses of rigid molecules, J. Chem. Phys. **53**, 2372 (1970).
[144] I. Chang and H. Sillescu, Heterogeneity at the glass transition: Translational and rotational self-diffusion, J. Phys. Chem. B **101**, 8794 (1997).
[145] R. Yamamoto and A. Onuki, Heterogeneous diffusion in highly supercooled liquids, Phys. Rev. Lett. **81**, 4915 (1998).
[146] R. Richert and R. Böhmer, Heterogeneous and homogeneous diffusivity in an ion-conducting glass, Phys. Rev. Lett. **83**, 4337 (1999).
[147] X. Xu, J. F. Douglas, and W.-S. Xu, Parallel emergence of rigidity and collective motion in a family of simulated glass-forming polymer fluids, Macromolecules **56**, 4929 (2023).
[148] K. Schmidt-Rohr and H. W. Spiess, Nature of nonexponential loss of correlation above the glass transition investigated by multidimensional NMR, Phys. Rev. Lett. **66**, 3020 (1991).
[149] F. H. Stillinger, Relaxation and flow mechanisms in "fragile" glass-forming liquids, J. Chem. Phys. **89**, 6461 (1988).
[150] S. K. Kumar, G. Szamel, and J. F. Douglas, Nature of the breakdown in the Stokes-Einstein relationship in a hard sphere fluid, J. Chem. Phys. **124**, 214501 (2006).
[151] G. Szamel and E. Flenner, Time scale for the onset of Fickian diffusion in supercooled liquids, Phys. Rev. E **73**, 011504 (2006).
[152] R. Higler, J. Krausser, J. van der Gucht, A. Zaccone, and J. Sprakel, Linking slow dynamics and microscopic connectivity in dense suspensions of charged colloids, Soft Matter **14**, 780 (2018).
[153] B. Guiselin, C. Scalliet, and L. Berthier, Microscopic origin of excess wings in relaxation spectra of supercooled liquids, Nat. Phys. **18**, 468 (2022).
[154] C. Scalliet, B. Guiselin, and L. Berthier, Thirty milliseconds in the life of a supercooled liquid, Phys. Rev. X **12**, 041028 (2022).
[155] I. M. Douglass and J. C. Dyre, Distance-as-time in physical aging, Phys. Rev. E **106**, 054615 (2022).
[156] J. C. Dyre, Solidity of viscous liquids. IV. Density fluctuations, Phys. Rev. E **74**, 021502 (2006).
[157] L. Gao, Y. Sun, and H.-B. Yu, Mobility percolation as a source of Johari-Goldstein relaxation in glasses, Phys. Rev. B **108**, 014201 (2023).
[158] C. Donati, J. F. Douglas, W. Kob, S. J. Plimpton, P. H. Poole, and S. C. Glotzer, Stringlike cooperative motion in a supercooled liquid, Phys. Rev. Lett. **80**, 2338 (1998).
[159] M. Russina, F. Mezei, R. Lechner, S. Longeville, and B. Urban, Experimental evidence for fast heterogeneous collective structural relaxation in a supercooled liquid near the glass transition, Phys. Rev. Lett. **84**, 3630 (2000).
[160] D. Long and F. Lequeux, Heterogeneous dynamics at the glass transition in van der Waals liquids, in the bulk and in thin films, Eur. Phys. J. E **4**, 371 (2001).
[161] J. D. Stevenson and P. G. Wolynes, A universal origin for secondary relaxations in supercooled liquids and structural glasses, Nat. Phys. **6**, 62 (2010).
[162] F. W. Starr, J. F. Douglas, and S. Sastry, The relationship of dynamical heterogeneity to the Adam-Gibbs and random first-order transition theories of glass formation, J. Chem. Phys. **138**, 12A541 (2013).
[163] M. T. Cicerone, Q. Zhong, and M. Tyagi, Picosecond dynamic heterogeneity, hopping, and Johari-Goldstein relaxation in glass-forming liquids, Phys. Rev. Lett. **113**, 117801 (2014).
[164] H.-B. Yu, R. Richert, and K. Samwer, Structural rearrangements governing Johari-Goldstein relaxations in metallic glasses, Sci. Adv. **3**, e1701577 (2017).
[165] B. A. P. Betancourt, F. W. Starr, and J. F. Douglas, String-like collective motion in the α- and β-relaxation of a coarse-grained polymer melt, J. Chem. Phys. **148**, 104508 (2018).
[166] F. Caporaletti, S. Capaccioli, S. Valenti, M. Mikolasek, A. I. Chumakov, and G. Monaco, A microscopic look at the Johari-Goldstein relaxation in a hydrogen-bonded glass-former, Sci. Rep. **9**, 14319 (2019).

[167] F. Caporaletti, S. Capaccioli, S. Valenti, M. Mikolasek, A. I. Chumakov, and G. Monaco, Experimental evidence of mosaic structure in strongly supercooled molecular liquids, Nat. Commun. **12**, 1867 (2021).

[168] C. Chang, H. P. Zhang, R. Zhao, F. C. Li, P. Luo, M. Z. Li, and H. Y. Bai, Liquid-like atoms in dense-packed solid glasses, Nat. Mater. **21**, 1240 (2022).

[169] F. Spieckermann, D. Sopu, V. Soprunyuk, M. B. Kerber, J. Bednarcik, A. Schökel, A. Rezvan, S. Ketov, B. Sarac, E. Schafler, and J. Eckert, Structure-dynamics relationships in cryogenically deformed bulk metallic glass, Nat. Commun. **13**, 127 (2022).

[170] V. N. Novikov, E. Rössler, V. K. Malinovsky, and N. V. Surovtsev, Strong and fragile liquids in percolation approach to the glass transition, Europhys. Lett. **35**, 289 (1996).

[171] Walter Kob, personal communication (2023).

[172] N. B. Olsen, Scaling of β-relaxation in the equilibrium liquid state of sorbitol, J. Non-Cryst. Solids **235**, 399 (1998).

[173] U. Schneider, R. Brand, P. Lunkenheimer, and A. Loidl, Excess wing in the dielectric loss of glass formers: A Johari-Goldstein β relaxation?, Phys. Rev. Lett. **84**, 5560 (2000).

[174] A. I. Nielsen, T. Christensen, B. Jakobsen, K. Niss, N. B. Olsen, R. Richert, and J. C. Dyre, Prevalence of approximate $\sqrt{t}$ relaxation for the dielectric α process in viscous organic liquids, J. Chem. Phys. **130**, 154508 (2009).

[175] F. Pabst, J. P. Gabriel, T. Böhmer, P. Weigl, A. Helbling, T. Richter, P. Zourchang, T. Walther, and T. Blochowicz, Generic structural relaxation in supercooled liquids, J. Phys. Chem. Lett. **12**, 3685 (2021).

[176] D. L. Sidebottom, Generic α relaxation in a strong GeO_2 glass melt, Phys. Rev. E **107**, L012602 (2023).

[177] C. Kittel, *Introduction to Solid State Physics, 5th Ed.* (Wiley, New York, 1976).

[178] C. P. Flynn, Atomic migration in monatomic crystals, Phys. Rev. **171**, 682 (1968).

[179] T. Rouxel, Thermodynamics of viscous flow and elasticity of glass forming liquids in the glass transition range, J. Chem. Phys. **135**, 184501 (2011).

[180] B. A. P. Betancourt, P. Z. Hanakata, F. W. Starr, and J. F. Douglas, Quantitative relations between cooperative motion, emergent elasticity, and free volume in model glass-forming polymer materials, PNAS **112**, 2966 (2015).

[181] S. Mirigian and K. S. Schweizer, Elastically cooperative activated barrier hopping theory of relaxation in viscous fluids. I. General formulation and application to hard sphere fluids, J. Chem. Phys. **140**, 194506 (2014).

[182] A. Phan and K. S. Schweizer, Elastically collective nonlinear Langevin equation theory of glass-forming liquids: Transient localization, thermodynamic mapping, and cooperativity, J. Phys. Chem. B **122**, 8451 (2018).

[183] B. Mei, Y. Zhou, and K. S. Schweizer, Experimental test of a predicted dynamics–structure–thermodynamics connection in molecularly complex glass-forming liquids, PNAS **118**, e2025341118 (2021).

[184] J. C. Dyre, A model for the generic alpha relaxation of viscous liquids, Europhys. Lett. **71**, 646 (2005).

[185] W. L. Johnson and K. Samwer, A universal criterion for plastic yielding of metallic glasses with a $(T/T_g)^{2/3}$ temperature dependence, Phys. Rev. Lett. **95**, 195501 (2005).

[186] S. S. Schoenholz, A. J. Liu, R. A. Riggleman, and J. Rottler, Understanding plastic deformation in thermal glasses from single-soft-spot dynamics, Phys. Rev. X **4**, 031014 (2014).

[187] J. C. Dyre, N. B. Olsen, and T. Christensen, Local elastic expansion model for viscous-flow activation energies of glass-forming molecular liquids, Phys. Rev. B **53**, 2171 (1996).

[188] T. Hecksher and J. C. Dyre, A review of experiments testing the shoving model, J. Non-Cryst. Solids **407**, 14 (2015).

[189] J. C. Dyre, Dominance of shear elastic energy far from a point defect in a solid, Phys. Rev. B **75**, 092102 (2007).

[190] P. A. Varotsos and K. D. Alexopoulos, *Thermodynamics of Point Defects and their Relation with Bulk Properties* (North-Holland, Amsterdam, 1986).

[191] R. W. Hall and P. G. Wolynes, The aperiodic crystal picture and free energy barriers in glasses, J. Chem. Phys. **86**, 2943 (1987).

[192] L. Larini, A. Ottochian, C. D. Michele, and D. Leporini, Universal scaling between structural relaxation and vibrational dynamics in glass-forming liquids and polymers, Nat. Phys. **4**, 42 (2008).

[193] J. Ding, Y.-Q. Cheng, H. Sheng, M. Asta, R. O. Ritchie, and E. Ma, Universal structural parameter to quantitatively predict metallic glass properties, Nat. Comm **7**, 13733 (2016).

[194] J. M. Lovi and S. Sen, Effects of the 10B/11B isotopic substitution on shear relaxation in supercooled B_2O_3 liquid: A validation of the elastic model of viscous flow, J. Chem. Phys. **158**, 141103 (2023).

[195] J. Dudowicz, K. F. Freed, and J. F. Douglas, The glass transition temperature of polymer melts, J. Phys. Chem. B **109**, 21285 (2005).

[196] U. R. Pedersen, L. Costigliola, N. P. Bailey, T. B. Schrøder, and J. C. Dyre, Thermodynamics of freezing and melting, Nat. Commun. **7**, 12386 (2016).

[197] P. Lunkenheimer, A. Loidl, B. Riechers, A. Zaccone, and K. Samwer, Thermal expansion and the glass transition, Nat. Phys. **19**, 694 (2023).

[198] J. C. Dyre and W. H. Wang, The instantaneous shear modulus in the shoving model, J. Chem. Phys. **136**, 224108 (2012).

[199] T. Scopigno, G. Ruocco, F. Sette, and G. Monaco, Is the fragility of a liquid embedded in the properties of its glass?, Science **302**, 849 (2003).

[200] A. A. Veldhorst and M. C. C. Ribeiro, Mechanical heterogeneity in ionic liquids, J. Chem. Phys. **148**, 193803 (2018).

[201] B. Shang, J. Rottler, P. Guan, and J.-L. Barrat, Local versus global stretched mechanical response in a supercooled liquid near the glass transition, Phys. Rev. Lett. **122**, 105501 (2019).

[202] P. Weigl, T. Hecksher, J. C. Dyre, T. Walther, and T. Blochowicz, Identity of the local and macroscopic dynamic elastic responses in supercooled 1-propanol, Phys. Chem. Chem. Phys. **23**, 16537 (2021).

[203] G. Kapteijns, D. Richard, E. Bouchbinder, T. B. Schrøder, J. C. Dyre, and E. Lerner, Does mesoscopic elasticity control viscous slowing down in glassforming liquids?, J. Chem. Phys. **155**, 074502 (2021).

[204] J. C. Dyre, Source of non-Arrhenius average relaxation

time in glass-forming liquids, J. Non-Cryst. Solids **235**, 142 (1998).

[205] S. Mirigian and K. S. Schweizer, Unified theory of activated relaxation in liquids over 14 decades in time, J. Phys. Chem. Lett. **4**, 3648 (2013).

[206] D. H. Torchinsky, J. A. Johnson, and K. A. Nelson, A direct test of the correlation between elastic parameters and fragility of ten glass formers and their relationship to elastic models of the glass transition, J. Chem. Phys. **130**, 064502 (2009).

[207] E. Flenner and G. Szamel, Fundamental differences between glassy dynamics in two and three dimensions, Nat. Commun. **6**, 7392 (2015).

[208] L. Berthier, P. Charbonneau, A. Ninarello, M. Ozawa, and S. Yaida, Zero-temperature glass transition in two dimensions, Nat. Commun. **10**, 1508 (2019).

[209] A. Vila-Costa, M. Gonzalez-Silveira, C. Rodriguez-Tinoco, M. Rodriguez-Lopez, and J. Rodriguez-Viejo, Emergence of equilibrated liquid regions within the glass, Nat. Phys. **19**, 114 (2023).

[210] D. Kong, W.-R. Chen, K.-Q. Zeng, L. Porcar, and Z. Wang, Localized elasticity governs the nonlinear rheology of colloidal supercooled liquids, Phys. Rev. X **12**, 041006 (2022).

[211] F. Vogel, A. Zippelius, and M. Fuchs, Emergence of Goldstone excitations in stress correlations of glass-forming colloidal dispersions, Europhys. Lett. **125**, 68003 (2019).

[212] C. Herrero, C. Scalliet, M. D. Ediger, and L. Berthier, Two-step devitrification of ultrastable glasses, PNAS **120**, e2220824120 (2023).

[213] K. Karimi, M. J. Alava, and S. Papanikolaou, Yielding in multicomponent metallic glasses: Universal signatures of elastic modulus heterogeneities, Phys. Rev. Mater. **7**, 063601 (2023).

[214] T. B. Schrøder and J. C. Dyre, Solid-like mean-square displacement in glass-forming liquids, J. Chem. Phys. **152**, 141101 (2020).

[215] S. P. Bierwirth, R. Böhmer, and C. Gainaru, Generic primary mechanical response of viscous liquids, Phys. Rev. Lett. **119**, 248001 (2017).